PLANAR CABLE-DIRECT-DRIVEN ROBOTS: DESIGN FOR WRENCH EXERTION

Robert L. Williams II[1]
Department of Mechanical Engineering
Ohio University
Athens, Ohio

Paolo Gallina[2]
Dipartimento di Innovazione Meccanica e Gestionale
University of Padova
Padova, Italy

Journal of Intelligent and Robotic Systems
Vol. 35, pp. 203-219
2002

Keywords: cable robot design, cable-direct-driven robots, actuation redundancy, cable interference, wrench-exertion workspace

ABSTRACT

Cable-direct-driven robots and haptic interfaces are appealing because of their structural simplicity, high stiffness, and high exerted wrench-to-weight ratio. A major drawback is that cables can only exert tension. Therefore, actuation redundancy is required to apply general wrenches (force/moment vectors). Even with actuation redundancy, not all desired wrenches can be applied in some configurations due to one or more negative cable forces required. In addition, cable interference can be a serious problem for these devices. The objective of this article is to present the best design for planar cable-direct-driven robots and/or haptic interfaces with one degree of actuation redundancy, with regard to general wrench exertion and cable interference. Results indicate that the cable interference constraint dominates which suggests the need for future design work to alleviate this interference.

[1] Associate Professor, Corresponding Author
[2] Assistant Professor

INTRODUCTION

Several cable-direct-driven robots (CDDRs) and haptic interfaces (CDDHIs) have been studied in the past. An early CDDR is the *Robocrane* developed by NIST for use in shipping ports (Albus, et. al., 1993). This device is similar to an upside-down six-degrees-of-freedom (dof) Stewart platform (Stewart, 1966), with six cables instead of hydraulic-cylinder legs. In this system, gravity is an implicit actuator that ensures cable tension is maintained at all times. Another CDDR is *Charlotte*, developed by McDonnell-Douglas (Campbell, et. al., 1992) for use on International Space Station. *Charlotte* is a rectangular box driven in-parallel by eight cables, with eight tensioning motors mounted on-board (one on each corner). Three stringed haptic interfaces have been built and tested, the *Texas 9-string* (Lindemann and Tesar, 1989), the *SPIDAR* (Ishii and Sato, 1994), and the 7-cable master (Kawamura and Ito, 1993). CDDRs and CDDHIs can be made lighter, stiffer, safer, and more economical than traditional serial robots and haptic interfaces since their primary structure consists of lightweight, high load-bearing cables. On the other hand, one major disadvantage is that cables can only exert tension and cannot push on the moving platform. All of the devices discussed above are designed with actuation redundancy, i.e. more cables than wrench-exerting degrees-of-freedom (except for the *Robocrane*, where tensioning is provided by gravity) in attempt to avoid configurations where certain wrenches require an impossible compression force in one or more cables. Despite actuation redundancy, there exist subspaces in the potential workspace where some cables can lose tension. Roberts et al. (1997) developed an algorithm for CDDRs to predict if all cables are under tension in a given configuration while supporting the robot weight only. None of these previous articles have presented CDDR or CDDHI design for optimal wrench exertion. Another potential problem with CDDRs and CDDHIs is cable interference that further restricts the workspace.

A haptic interface is a device that can exert wrench (force/moment) and/or tactile feedback to the human from virtual reality and/or remote environments. The current article focuses on wrench feedback. Many researchers have been developing haptic interfaces for various applications. A comprehensive study of force-, wrench-, and tactile-feedback haptic interfaces is provided by Burdea (1996).

The objective of the current article is to present the best design for CDDRs and CDDHIs with one degree of actuation redundancy, with regard to best general wrench exertion and with regard to avoiding cable/end-effector interference. Specifically, this article focuses on the planar 3-dof, 4-cable CDDR that is required to exert general wrenches on the environment. This work equally applies to CDDHIs with one degree of actuation redundancy that must exert general wrenches on the human operator's hand.

This article begins with a description of the planar CDDR, followed by CDDR cable interference determination, statics modeling, a method for attempting to maintain positive cable tensions, and then design and results for planar CDDRs with one actuation redundancy, considering both positive cable tensions and cable interference.

LIST OF SYMBOLS

x, y, ϕ	Cartesian parameters of end-effector
$\{0\}, \{H\}$	Fixed base and moving end-effector Cartesian coordinate frames
a, b, c	end-effector width, end-effector height, and square ground link side
L_i , $\hat{L}_i$	i^{th} cable length, unit vector in the L_i direction
w_{fc}	Cable-interference-free workspace
h_i , T_i	i^{th} cable end-effector connection point, i^{th} cable ground connection point
${}^{+}v_i$ and ${}^{-}v_i$	unit directions of two consecutive edges of end-effector
$\left\lfloor {}^{o}_{H}R \right\rfloor$	Orthonormal rotation matrix relating $\{H\}$ to $\{0\}$
f_i	i^{th} cable force
$\{W_R\} = \{\underline{F}_R \quad \underline{M}_R\}^T$	Cartesian wrench exerted on the environment by end-effector
$[A]$, $[A]^+$	Statics Jacobian matrix, Moore-Penrose pseudoinverse of $[A]$
n_i	i^{th} component of the kernel vector of $[A]$
α	Scalar for tension optimization

PLANAR CABLE-DIRECT-DRIVEN ROBOT (CDDR)

This section describes the planar 4-cable CDDR, includes a brief discussion on CDDR kinematics, and presents a general model to determine cable/end-effector interference.

A CDDR consists of a rigid end-effector supported in-parallel by *n*-cables controlled by *n* tensioning actuators. Figure 1 shows the planar 4-cable CDDR kinematics diagram. For 3-dof planar operation, there must be at least 3 cables. Since cables can only exert tension on the end-effector, there must be more cables to avoid configurations where the end-effector can go slack and lose control. Our work is limited to CDDRs with one degree of actuation redundancy, i.e. 4 cables in planar devices with 3 Cartesian degrees-of-freedom. This scenario represents actuation redundancy but not kinematic redundancy. That is, there is one extra motor which provides infinite choices for applying 3-dof wrench vectors, but the end-effector has only 3 Cartesian degrees-of-freedom (x, y, ϕ; angle ϕ is shown in Fig. 1 and x, y are the components of the vector from the origin of $\{0\}$ to the origin of $\{H\}$, expressed in $\{0\}$). Figure 1 shows the definitions for reference frame $\{0\}$ and moving end-effector frame $\{H\}$. In Fig. 1, the design parameters for the planar 4-cable CDDR are a (end-effector width), b (end-effector height), and c (square ground link side). The length of each cable is denoted as L_i, i = 1,2,3,4.

Planar CDDR Kinematics

This section briefly discusses the required kinematics solutions. Assuming all cables always remain in tension, CDDR kinematics is similar to in-parallel-actuated robot kinematics (e.g. Tsai, 1999; Gosselin, 1996). In CDDR simulation for design, the inverse pose kinematics solution is straight-forward (given the pose, calculate the cable lengths). The forward kinematics problem requires the solution of overconstrained coupled nonlinear equations and is more difficult. A Newton-Raphson numerical solution is employed, where the overconstrained Moore-Penrose pseudoinverse is used in the iteration. The CDDR inverse velocity Jacobian matrix is closely related to the Newton-Raphson Jacobian matrix and the statics Jacobian matrix. These kinematics solutions are presented in (Williams, 1998).

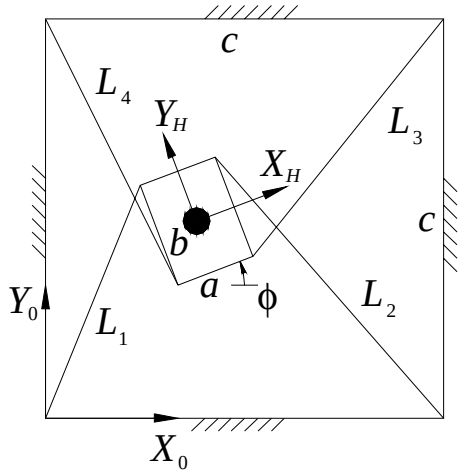

Figure 1. Planar 4-Cable CDDR Kinematics Diagram

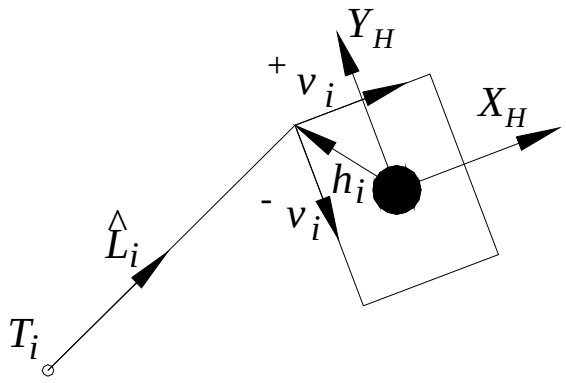

Figure 2. Cable/End-effector Interference Diagram

Planar CDDR Cable Interference

A potential workspace-limiting problem for CDDRs is that of cable interference. This can take three forms: cable/cable interference, cable/workspace object interference, or cable/end-effector interference. In the planar case we can easily avoid the former case by designing the device so all cables are in different parallel planes. Also, the cable/ workspace object interference will not be a problem for the planar case if all objects are below (or above the plane of the CDDR). We cannot always avoid by design the latter interference and thus we present in this section a method for determining cable/end-effector collisions.

Let us define collision- free workspace w_{fc} as the subset of workspace that can be reached without collision between the end-effector and the cables. In the following we assume that the end-effector is a convex polygon and that all cables are attached to the polygon vertices. The aim of this section is to develop a method for checking whether a end-effector configuration $\{x \quad y \quad \phi\}$ belongs to w_{fc}. Let us define ${}^{+}\phi$ as the angular value that the end-effector can rotate anticlockwise before a collision. Conversely, let us define ${}^{-}\phi$ as the angular value that the end-effector can rotate clockwise before a collision. Note that these limiting angles depend on the position $\{x \quad y\}$ and they take into account all cables.

Let us consider the i^{th} cable in the cable/end-effector diagram of Fig. 2. The unit vector in the direction of the i^{th} cable is $\hat{L}_i$. The cable is connected to the end-effector at point h_i (Fig. 2 shows the vector h_i to this point, referenced to the moving $\{H\}$ frame). For each point h_i we define two vectors ${}^{+}v_i$ and ${}^{-}v_i$ that represent the unit directions of two consecutive edges of the polygon. A collision occurs when the cable direction aligns with one of the neighboring consecutive polygon faces, i.e.:

$$\hat{L}_i = -{}^{+}v_i \qquad or \qquad \hat{L}_i = -{}^{-}v_i \tag{1}$$

The negative signs in (1) indicate that at collision the cable direction is aligned but opposite in direction to the polygon face. Define T_i as the grounded point for the i^{th} cable and $G = \{x \quad y\}^T$ as the origin of $\{H\}$, expressed in $\{0\}$. Then the collision conditions (1) can be expressed as:

$$T_i - \left(\left[{}^{o}_{H}R \right]^{H} h_i + G \right) = \lambda \left[{}^{o}_{H}R \right]^{H} {}^{+}v_i \qquad or \qquad T_i - \left(\left[{}^{o}_{H}R \right]^{H} h_i + G \right) = \lambda \left[{}^{o}_{H}R \right]^{H} {}^{-}v_i \tag{2}$$

where: $\lambda = \left\| T_i - \left(\left[{}^{o}_{H}R \right]^{H} h_i + G \right) \right\|$ and $\left[{}^{o}_{H}R \right] = \begin{bmatrix} \cos\phi & -\sin\phi \\ \sin\phi & \cos\phi \end{bmatrix}$

By introducing a new vector $m = \{m_{ix} \quad m_{iy}\}^T = T_i - G$, equations (2) yield:

$$\begin{cases} {}^{+/-}v_{ix}\lambda + h_{ix} = \cos\phi\, m_{ix} + \sin\phi\, m_{iy} \\ {}^{+/-}v_{iy}\lambda + h_{ix} = -\sin\phi\, m_{ix} + \cos\phi\, m_{iy} \end{cases} \tag{3}$$

where the symbol ${}^{+/-}v_{ix}$ indicates that there are two possibilities, one with ${}^{+}v_{ix}$ and one with ${}^{-}v_{ix}$. All possible solutions of (3) are given by:

$$\phi = \pm \arccos\left(\frac{AB \pm \sqrt{C^4 + B^2C^2 - A^2C^2}}{B^2 + C^2} \right) \tag{4}$$

where:

$$A=\frac{h_{ix}}{{}^{+/-}v_{ix}}-\frac{h_{iy}}{{}^{+/-}v_{iy}} \quad B=\frac{m_{ix}}{{}^{+/-}v_{ix}}-\frac{m_{iy}}{{}^{+/-}v_{iy}} \quad C=\frac{m_{ix}}{{}^{+/-}v_{iy}}+\frac{m_{iy}}{{}^{+/-}v_{ix}} \qquad if\ {}^{+/-}v_{ix}\neq 0, {}^{+/-}v_{iy}\neq 0$$

$$A=h_{ix} \quad B=m_{ix} \quad C=m_{iy} \qquad if\ {}^{+/-}v_{ix}=0$$

$$A=h_{iy} \quad B=m_{iy} \quad C=-m_{ix} \qquad if\ {}^{+/-}v_{iy}=0$$

From (4) we obtain 4 values for each of the two ${}^{+/-}v_{ix}$, but only one of them satisfies (3) and at the same time yields positive λ. It is straight-forward to implement this cable/end-effector algorithm in a computer program. Let us indicate these solutions as ${}^{+}\phi_i$ if we consider ${}^{+}v_{ix}$ and ${}^{-}\phi_i$ if we consider ${}^{-}v_{ix}$. Notice that ${}^{+}\phi_i$ has to be positive while ${}^{-}\phi_i$ has to be negative. In conclusion:

$$\begin{aligned} {}^{+}\phi &= \min\left\{{}^{+}\phi_1,...,{}^{+}\phi_n\right\} \\ {}^{-}\phi &= \max\left\{{}^{-}\phi_1,...,{}^{-}\phi_n\right\} \end{aligned} \tag{5}$$

gives the limiting angles for cable/end-effector interference considering all cables $i=1,2,\cdots,n$; where $n=4$ in this article.

CDDR STATICS

In this article, the workspace wherein all cables are under positive tension while exerting all possible wrenches is called the statics workspace. The wrench is a force and moment applied to the environment, centered at the origin of the end-effector frame $\{H\}$; this is different from a wrench definition where the moment is about the base frame $\{0\}$. We assume velocities and accelerations on the end-effector are small and thus the device may be controlled in a pseudostatic manner. Statics modeling and attempting to maintain positive cable tension are presented in this section. We use a simple method to determine the extent of the statics workspace, i.e. the workspace wherein all possible wrenches can be applied with only positive cable tension.

Statics Modeling

This section presents statics modeling for planar CDDRs. For static equilibrium the sum of external forces and moments exerted on the end-effector by the cables must equal the resultant external wrench exerted on the environment. Figure 3 shows the statics free-body diagram for the planar 4-cable CDDR.

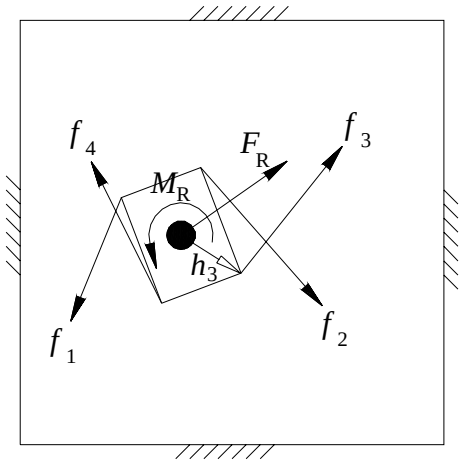

Figure 3. Planar 4-Cable CDDR Statics Diagram

The statics equations are:

$$\sum_{i=1}^{4} \underline{f}_i = -\sum_{i=1}^{4} f_i \hat{L}_i = \underline{F}_R \qquad \sum_{i=1}^{4} \underline{m}_i = \sum_{i=1}^{4} \left(\left[{}^{0}_{H}R \right] \underline{h}_i \right) \times \underline{f}_i = \underline{M}_R \tag{6}$$

In this article gravity is ignored because it is assumed to be perpendicular to the CDDR plane; we assume the end-effector is supported on a plane. The definition of frames $\{0\}$ and $\{H\}$ are given in Fig. 1. In (6), f_i is the

cable tension applied to the i^{th} cable (in the negative cable length unit direction $\hat{L}_i$ because $\underline{f}_i$ must be in tension); $\left[{}^{O}_{H}R\right]$ is the rotation matrix relating the orientation of {*H*} to {0}; $\underline{h}_i$ is the position vector from the origin of {*H*} to the i^{th} cable connection, expressed in {*H*} (only $\underline{h}_3$ is shown in Fig. 3); and $\underline{F}_R$ and $\underline{M}_R$ are the resultant vector force and moment (taken together, wrench) exerted on the environment. Again, let us emphasize that this wrench acts at the end-effector frame {*H*} origin. Substituting the above terms into (6) yields:

$$[A]\{f\}=\{W_R\} \tag{7}$$

where $\{f\}=\{f_1 \quad f_2 \quad f_3 \quad f_4\}^T$ is the vector of scalar cable forces, $\{W_R\}=\{\underline{F}_R \quad \underline{M}_R\}^T=\{F_x \quad F_y \quad M_z\}^T$ is the resultant external wrench vector exerted on the environment by the end-effector (expressed in {*0*} coordinates but felt at the origin of {*H*}), and the 3*x*4 Statics Jacobian matrix $[A]$ (expressed in {*0*} coordinates) is:

$$[A]=\begin{bmatrix} -\hat{L}_1 & -\hat{L}_2 & -\hat{L}_3 & -\hat{L}_4 \\ \hat{L}_1\times\left[{}^{0}_{H}R\right]\underline{h}_1 & \hat{L}_2\times\left[{}^{0}_{H}R\right]\underline{h}_2 & \hat{L}_3\times\left[{}^{0}_{H}R\right]\underline{h}_3 & \hat{L}_4\times\left[{}^{0}_{H}R\right]\underline{h}_4 \end{bmatrix} \tag{8}$$

The statics equations (7) can be inverted in an attempt to exert general wrenches while maintaining positive cable tension. This work is presented in the next subsection.

Maintaining Positive Cable Tension

For CDDRs with actuation redundancy, (7) is underconstrained which means that there are infinite solutions to the cable force vector $\{f\}$ to exert the given wrench $\{W_R\}$. Roberts et al. (1997) present a method for determining if a vector of only positive cable forces exists for CDDRs under gravity loading only. This algorithm could be extended to CDDRs with general wrench exertion, but for the planar 4-cable case with only one degree of actuation redundancy, a simpler method is used here, based on Shen et al. (1994).

First, to invert (7) (solving the required cable tensions $\{f\}$ given the desired wrench $\{W_R\}$) we adapt the well-known particular and homogeneous solution from rate control of kinematically-redundant manipulators:

$$\{f\}=[A]^{+}\{W_R\}+\left([I_4]-[A]^{+}[A]\right)\{z\} \tag{9}$$

where $[I_4]$ is the 4*x*4 identity matrix, $\{z\}$ is an arbitrary 4-vector, and $[A]^+ = [A]^T \left([A][A]^T\right)^{-1}$ is the 4*x*3 Moore-Penrose pseudoinverse of $[A]$. The first term of (9) is the particular solution to achieve the desired wrench, and the second term is the homogeneous solution that maps $\{z\}$ to the null space of $[A]$. For actuation redundancy of degree one, an equivalent expression for (9) is:

$$\{f\} = \begin{Bmatrix} f_{P1} \\ f_{P2} \\ f_{P3} \\ f_{P4} \end{Bmatrix} + \alpha \begin{Bmatrix} n_1 \\ n_2 \\ n_3 \\ n_4 \end{Bmatrix} \tag{10}$$

where the particular solution $[A]^+\{W_R\}$ is the first term in (10) and the homogeneous solution is expressed as the kernel vector of $[A]$ ($N = \{n_1 \quad n_2 \quad n_3 \quad n_4\}^T$) multiplied by an arbitrary scalar α.

The method we adapt from Shen et al. (1994) to determine if a given configuration lies within the statics workspace for a given CDDR design is simple. To ensure positive tensions f_i on all cables i = 1,2,3,4 *for all possible exerted wrenches*, it is necessary and sufficient that all kernel vector components (n_i, i = 1,2,3,4) have the same sign. That is, for a given configuration of a given CDDR design to lie within the statics workspace, all $n_i > 0$ OR all $n_i < 0$ (i = 1,2,3,4). If one of these two conditions is satisfied, regardless of the particular solution, we can find a scalar α in (10) which guarantees that all cable tensions $\{f\}$ are positive by adding (or subtracting) enough homogeneous solution. Note a strict inequality is required; if one or more $n_i = 0$, the configuration in question does not lie within the statics workspace. This method is simple but powerful since we needn't consider specific wrenches, but it works for *all possible wrenches*. It should be noted that this method is necessarily conservative, i.e. there may exist combinations of positive and negative particular and homogeneous solution components that may yield positive cable tensions by proper choice of α for a certain wrench, but our goal in design is to ensure that *all possible wrenches* be satisfied in the statics workspace, not merely some wrenches. It should also be noted that while we demonstrate this method for the planar 4-cable CDDR, it is

applicable to any CDDR with one degree of actuation redundancy. Also, there is no guarantee that scalar α in (10) exists to guarantee that all cable tensions $\{f\}$ are positive; in fact, when such α ceases to exist, this defines the boundary of the statics workspace.

For design purposes we need to calculate this kernel vector repeatedly, for many CDDR designs and many configurations within each design. Equation (11) gives the method to calculate each kernel vector component n_i, where $|A_i|$ is the determinant of the 3*x*3 submatrix of $[A]$ with column *i* removed.

$$n_i = (-1)^{i+1}|A_i| \qquad i = 1,2,3,4 \qquad (11)$$

For on-line control purposes, once a given wrench at a given configuration is determined to be feasible via the above-described method, the tensions for control are calculated by (10), choosing α so that one component of $\{f\}$ is zero (or, a small positive value) and the remaining terms are positive. Of course, if the particular solution happens to contain all positive terms then α can be chosen to be 0; alternatively in this case, α can still be chosen so that one component of $\{f\}$ is zero (or, a small positive value), which results in the same Cartesian wrench but lower cable tensions.

PLANAR CDDR DESIGN RESULTS

This section presents the parameters, design process, and results for determining the best CDDR design with regard to wrench exertion and cable interference. In previous computer simulations (Williams, 1998), it was discovered that the planar crossed-cable case (Fig. 1) was far superior to the planar non-crossed-cable case (not shown), particularly in exerting moments. Therefore we only consider crossed cables in this article.

Planar 4-Cable CDDR Parameters

Assuming a square ground link, there are only three design parameters for the 4-cable planar CDDR: end-effector rectangular dimensions *a* and *b*, plus square ground link side *c* (refer to Fig. 1). If we normalize with *c* = 1 (the results may be scaled as needed), we have two design parameters *a* and *b*. In this article we limit *a* and *b* to the same ranges, $a,b \in [0.0 \quad 0.4]$. Note *a* = *b* = 0 is not a feasible design but we allow this case in our work for completeness; the results will show this case is in fact the least optimal design.

For the Cartesian plane we consider ϕ rotation at a grid of *XY* points covering $X,Y \in [0.2 \quad 0.8]$, determined by fitting the largest design [*a*, *b*] = [0.4 0.4] in the corners of the ground link square with *c* = 1.

Considering pitch ranges of the human wrist (when the hand grasps a cylindrical end-effector mounted perpendicular to the rectangular [*a*, *b*] end-effector at the center), a nominal desired rotation range is $\phi = \pm 45^\circ$. We wish to satisfy this statics workspace design requirement at all *XY* points for all applied wrenches.

Example Statics and Cable Interference Workspaces

An example statics workspace result is shown for planar CDDR design location (*a*, *b*) = (0.2, 0.3), *c* = 1 in the contour plots of Figs. 4. Figures 4 were generated using the kernel vector method described in the last section. Figure 4a shows the positive limiting angles $+\phi_T$ (the subscript *T* indicates tension) reachable at all *XY* locations considering only positive cable tensions, *for all possible exerted wrenches*. For certain wrenches, $+\phi_T$ will be larger at certain *XY* locations; however, we can guarantee *all possible wrenches* may be satisfied in the Fig. 4a statics workspace, again for only the positive cable constraint. Note that Fig. 4a demonstrates polar symmetry, as all such plots for any (*a*, *b*) design does: choose any value $+\phi_T$ in the *XY* plane and you will find the

identical value at the same radius from the center point (X, Y) = (0.5, 0.5) and directly opposite the chosen point. Also for this type of plot, the maximum possible $+\phi_T$ always occurs at the center point (X, Y) = (0.5, 0.5).

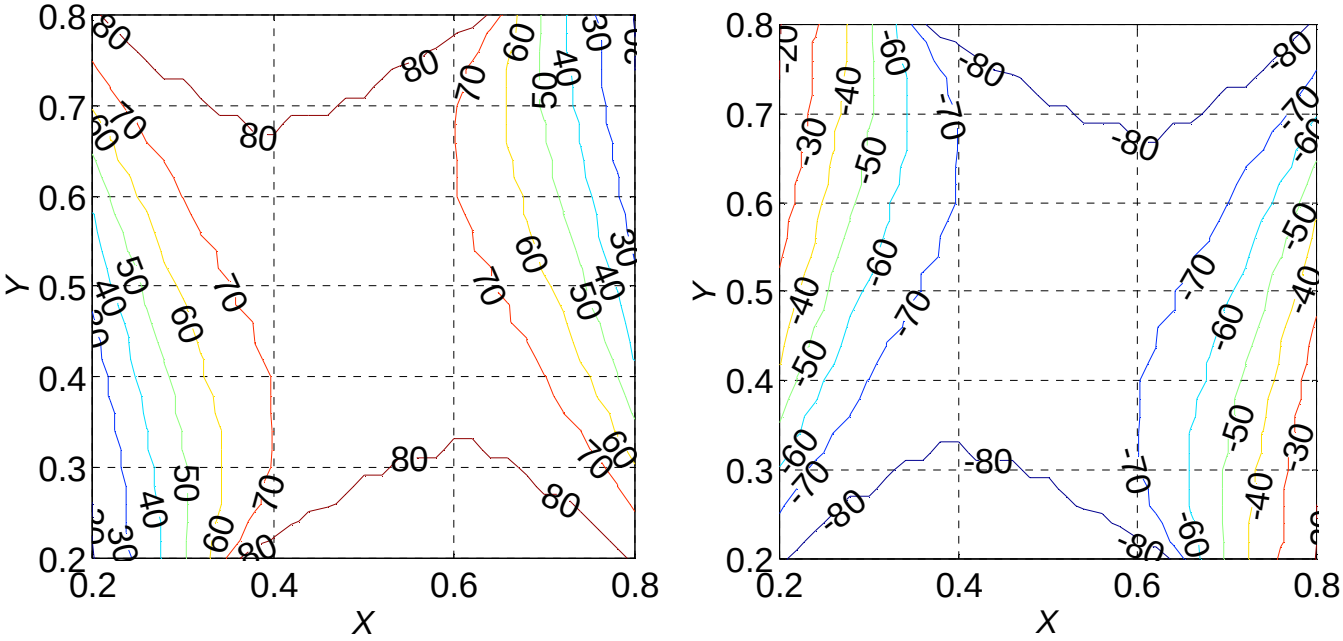

a. $+\phi_T$ *Contour (deg)* *b.* $-\phi_T$ *Contour (deg)*

Figure 4. Example Statics Workspace: Limiting Angle ϕ_T *Results over XY Plane* a = 0.2, b = 0.3, c = 1, *For All Possible Wrenches*

Comparing Fig. 4b to Fig. 4a, the $-\phi_T$ static workspace results can always be obtained by rotating the $+\phi_T$ results about the vertical line X = 0.5; thus we need only consider the $+\phi_T$ attribute for design purposes and then $-\phi_T$ will have the same values, mirrored about X = 0.5. From plots such as Fig. 4a, we can record the maximum, average, and minimum limiting angles over all XY. We will then use these measures to compare different (a, b) designs. For the example in Fig. 4a, MAX($+\phi_T$) = 90° (not visible in Fig. 4a since these occur only at discrete points), AVG($+\phi_T$) = 66.6°, and MIN($+\phi_T$) = 19.8°. Due to the vertical-mirrored symmetry, these measures are identical for Fig. 4b (where MAX now indicates the maximum negative angle): MAX($-\phi_T$) = -90° (again, not visible in Fig. 4b since these occur only at discrete points), AVG($-\phi_T$) = -66.6°, and MIN($-\phi_T$) = -19.8°. The MAX result is for a single XY point, always the middle of the XY workspace; due to symmetry, the MIN result occurs at two points, the lower-left and upper-right XY corners for $+\phi_T$, switching to the upper-left and lower-right XY corners for $-\phi_T$; the AVG result is for all XY.

For CDDR design, Figs. 4 are important to determine feasible statics workspaces wherein all possible wrenches can be exerted using only feasible (positive) cable tensions. However, this type of plot does not give the full story since cable interference may be important in CDDR design as well. As mentioned in the cable interference theory section, we only consider cable/end-effector interference since cable/cable interference may easily be avoided for planar CDDRs by arranging all cables in different planes, and cable/human interference is not a problem in the planar case. For the same planar CDDR design as Figs. 4 ((*a*, *b*) = (0.2, 0.3), *c* = 1), Fig. 5 shows the positive limiting angles $+\phi_C$ (the subscript *C* indicates collision) over all *XY* for cable/end-effector interference. Figure 5 reports a kinematic constraint of interference between the end-effector and any one of the four cables and hence is not related to the exerted wrenches. Figure 5 was generated using the cable/end-effector interference method presented earlier. Figure 5 demonstrates the same polar symmetry that Figs. 4 have. Again, the maximum $+\phi_C$ is in the middle of the workspace ((*X*, *Y*) = (0.5, 0.5)), as was the case for Figs. 4. Also, the negative limiting angles $-\phi_C$ may be obtained by exploiting the same symmetry between Figs. 4b and 4a: rotate the $+\phi_C$ results about the vertical line *X* = 0.5 to get the $-\phi_C$ contour (not shown). Thus, we need consider only the $+\phi_C$ attribute for design.

Again we record the MAX, AVG, and MIN values over all *XY* for design purposes: from Fig. 5, MAX($+\phi_C$) = 36.9°, AVG($+\phi_C$) = 24.4°, and MIN($+\phi_C$) = 7.1°. Due to the vertical-mirrored symmetry, the negative angle measures are identical, with a negative sign. Again, The MAX result is always for the middle of the *XY* workspace; the MIN result occurs at the lower-left and upper-right *XY* corners for $+\phi_C$, switching to the upper-left and lower-right *XY* corners for $-\phi_C$; the AVG result is again for all *XY*.

Comparing Figs. 4a and 5, it is clear that the cable/end-effector interference constraint dominates and its associated MAX, AVG, and MIN limiting angle values $+\phi_C$ are much less than those of $+\phi_T$. However, the statics workspace concept is still crucial for CDDRs since we are limited to feasible (positive) cable tensions. Therefore, we will consider both statics workspace and kinematics interference workspace in CDDR design.

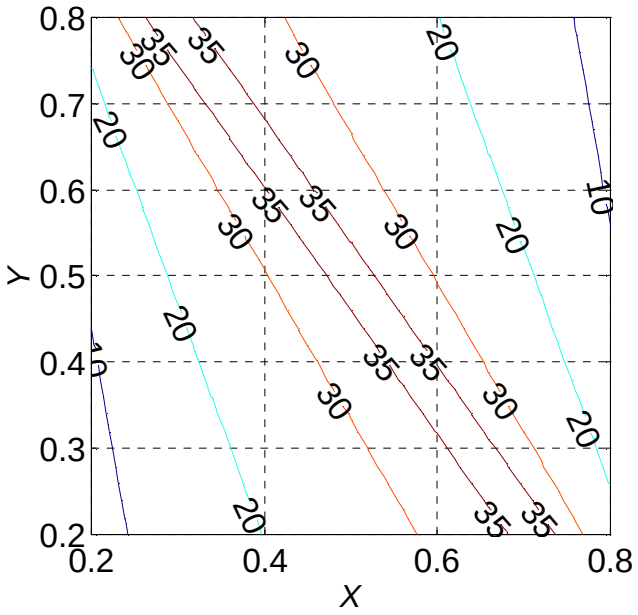

Figure 5. Example Interference Workspace: Limiting Angle $+\phi_C$ Results (deg) over XY Plane
$a = 0.2$, $b = 0.3$, $c = 1$

Planar 4-Cable CDDR Design Curves

We now present design curves to aid in selecting the best planar CDDR design, considering both positive cable tensions for all possible exerted wrenches and kinematic cable/end-effector interference.

Figures 6 show the MAX, AVG, and MIN $+\phi_T$ values over the design plane (a,b). Remember, due to symmetry, we needn't consider $-\phi_T$ separately. Figures 6 consider only the statics workspace constraint that all cable tensions must remain positive for exerting all possible wrenches. Each (a,b) location in Figs. 6 report the MAX, AVG, and MIN $+\phi_T$ (respectively), *each instance considering all XY locations*. That is, for each (a,b), a contour plot similar to Fig. 4a was generated and the computer program memorized the MAX, AVG, and MIN $+\phi_T$ values for later plotting against the a,b design plane. The program then iterated over all (a,b) locations under consideration. Design parameters a and b were each varied from 0 to 0.4 (with $c = 1$), in steps of 0.02. At each (a,b) location, X and Y were each varied from 0.2 to 0.8, in steps of 0.02 (these were also the parameters used in Figs. 4). Note a, b, c, X, and Y all have units of length; the results may be scaled as needed for CDDR design, based on the normalized $c = 1$.

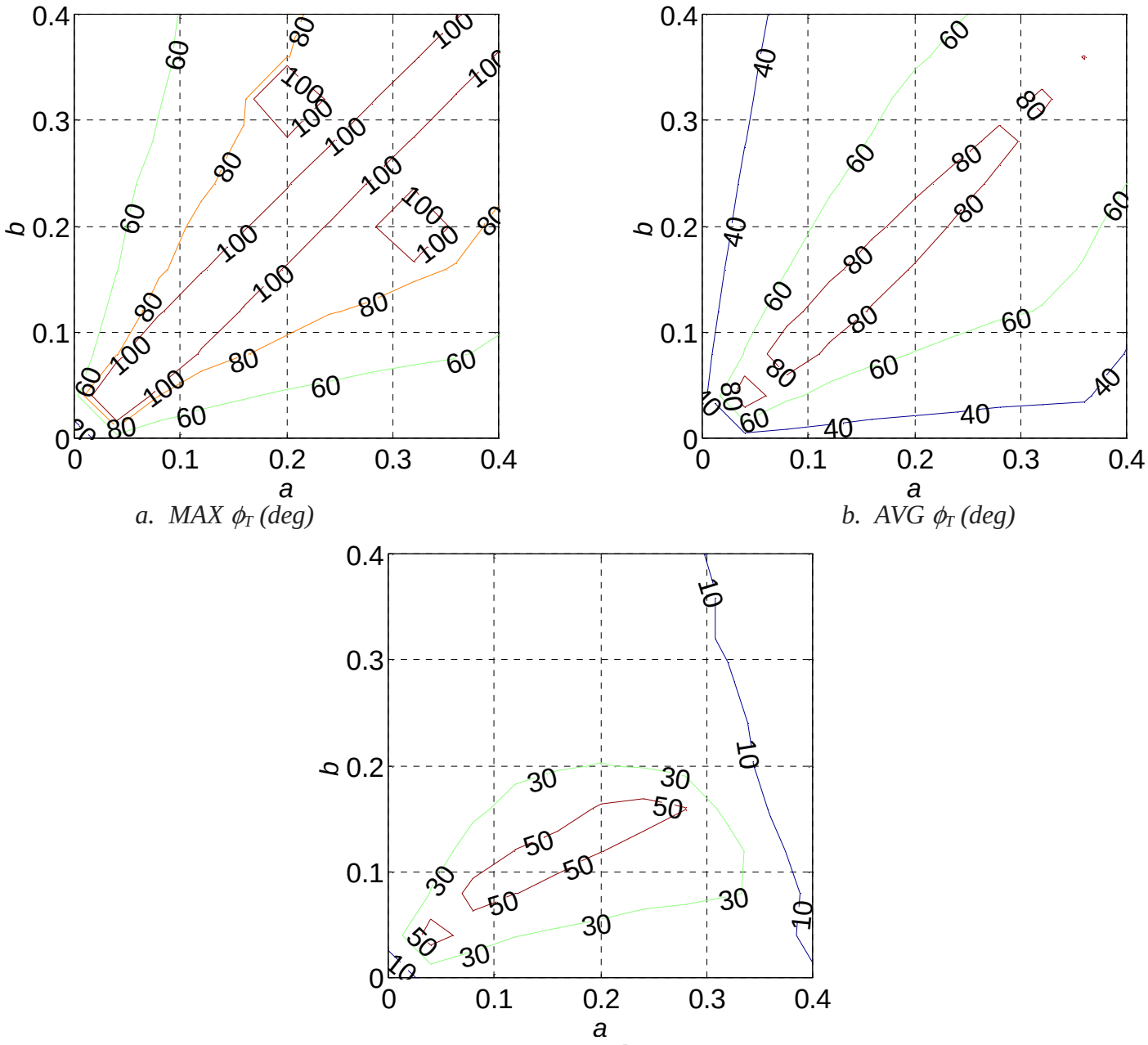

a. MAX ϕ_T (deg)

b. AVG ϕ_T (deg)

c. MIN ϕ_T (deg)

Figure 6. Design Curves, Tension Only: Limiting Angle ϕ_T Results over a, b Parameters

The MAX $+\phi_T$ results in Fig. 6a demonstrate a different type of symmetry than Figs. 4 and 5, about the *a* = *b* line. The AVG $+\phi_T$ results of Fig. 6b almost share this symmetry, but are off due to the lack of symmetry in the MIN $+\phi_T$ results of Fig. 6c. The MIN results are not symmetric due to the end-effector vertices rotating outside of the *XY* plane under consideration when the end-effector is placed at the lower-left and upper-right corners (where the MIN $+\phi_T$ values occur). Considering the statics workspace constraint only, the best designs

appear to be along the $a = b$ line toward the center of the a,b range. For good CDDR design, the AVG measure is more important than the MAX and MIN measures, since the latter two only involve one or two *XY* points, while the former involves all *XY* points.

We must also consider cable/end-effector interference in planar CDDR design. Another set of design curves was generated in the same manner as for Figs. 6, but this time considering only the kinematic cable-end-effector interference constraint. Three contour plots over all design parameters a,b were generated, showing the MAX, AVG, and MIN $+\phi_C$ limiting angles (again, $-\phi_C$ needn't be considered separately due to symmetry). These contour lines in all three cases were vertical; that is, for a given value of a, the limiting values ϕ_C remain unchanged for all possible b values. This behavior is expected since the end-effector height b does not affect the interference but the end-effector width a does.

This set of design curves for cable/end-effector interference only is not shown because they are so similar to the next set of design curves shown: the limiting cases are found over all a, b considering both statics workspace and interference constraints. That is, the statics-workspace-only design curves of Fig. 6 were compared with the kinematics-interference-only design curves (not shown) and the lesser value of the limiting angles reported (the smaller of ϕ_T and ϕ_C at each a, b design point), called ϕ_{TC} to indicate the limiting angle considering both tension and collision. Figures 7 show these *Overall Design Curves*, including the MAX, AVG, and MIN limiting angles ϕ_{TC} over all a, b design parameters under consideration. With the exception of the lower-left and lower-right corners of the a, b design plane, the interference constraint dominates.

Figures 7 show the limiting angle ϕ_{TC} MAX, AVG, and MIN values that can be obtained by planar CDDRs at the a, b design choices shown, considering both statics workspace and kinematics cable/end-effector interference constraints. To choose the best and worst planar CDDR designs we use the following procedure. Over all a, b we use a weighted sum of the MAX, AVG, and MIN ϕ_{TC} values, each normalized to have a largest value of 1.0 to make each equal in importance; further choosing an equal weighting between MAX, AVG, and

MIN yields the *Final Design Curve* shown in Fig. 8. A perfect score would be 3.0 (highest MAX, AVG, and MIN ϕ_{TC} all occurring at the same a, b value), while the worst score would be 0.0.

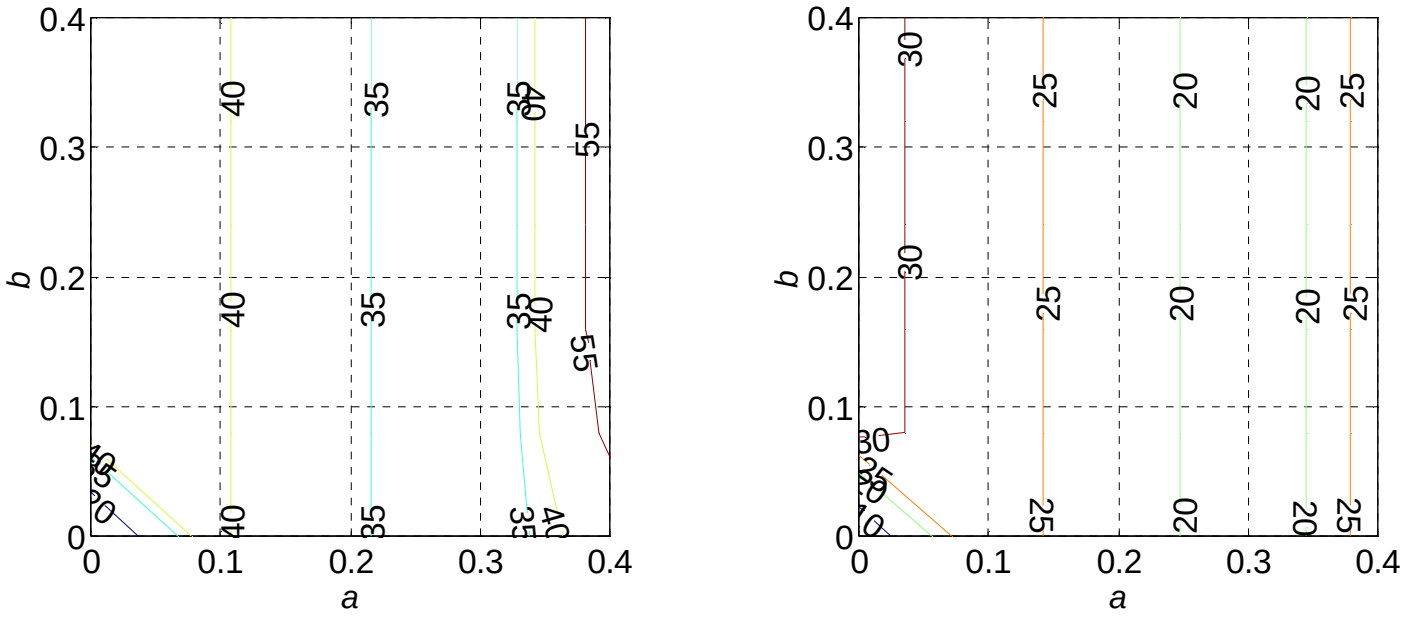

a. MAX ϕ_{TC} (deg) *b. AVG ϕ_{TC} (deg)*

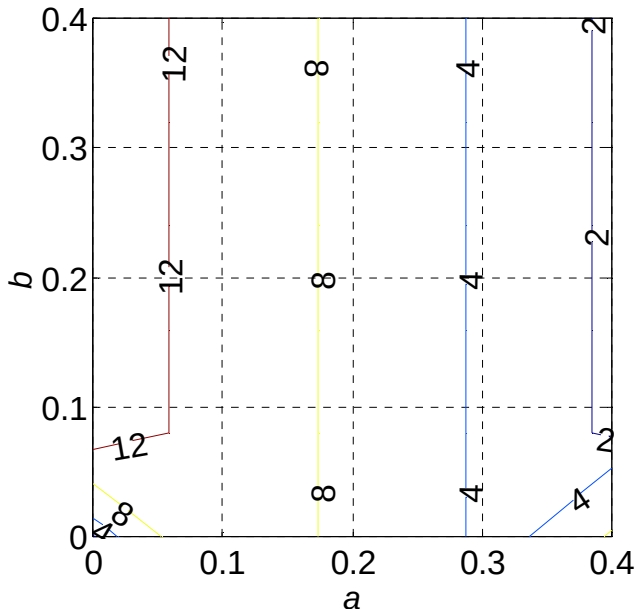

c. MIN ϕ_{TC} (deg)

Figure 7. Overall Design Curves considering both Tension and Collision

From Fig. 8, the best planar CDDR designs occur at $a = 0$ and $b > 0.1$ where the score is approximately 2.7. The worst design, as predicted, is at $a = b = 0$, which is an infeasible design; here the score approaches 0. The next-worst design lies along $a = 0.32$, where the score is approximately 1.2. Therefore we choose:

BEST design: $a = 0.0$ $b = 0.1$

WORST design: $a = 0.32$ $b = 0.05$

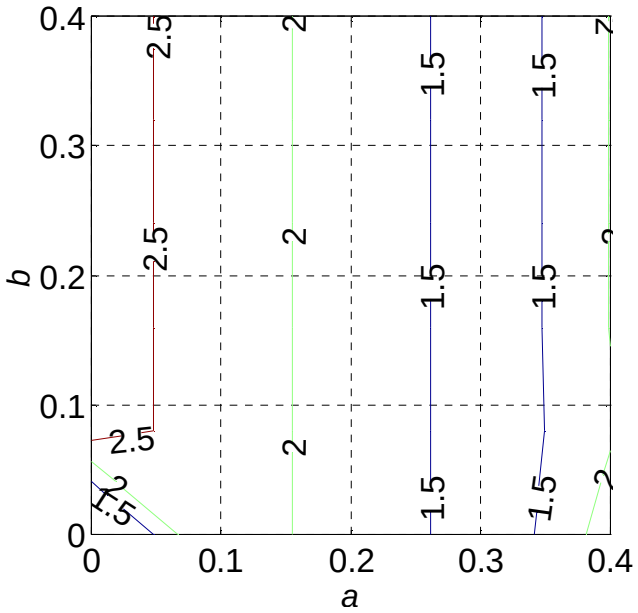

Figure 8. Final Design Curve considering both Tension and Collision and Equally Weighting MAX, AVG, and MIN Limiting Angles

Earlier we said that the AVG ϕ_{TC} value is the most important for planar CDDR design since it represents all possible *XY* locations, while the MAX is for the center point only and the MIN is for two corner points only. If one were to weight the results to use AVG only and ignore MAX and MIN, one would obtain nearly the same results as given above (see Fig. 7b to verify this fact).

Note that the general case chosen for detailed demonstration in Figs. 4 and 5 ($a = 0.2$, $b = 0.3$) was neither the best nor worst case, with an intermediate score of approximately 1.8.

BEST and WORST Results

Figure 9a shows the **BEST** planar CDDR design and Fig. 9b shows the associated achievable limiting angles ϕ_{TC} considering both statics workspace and kinematics cable/end-effector interference constraints. For comparison, Fig. 10a shows the **WORST** planar CDDR design and Fig. 10b shows the associated achievable limiting angles ϕ_{TC} considering both statics workspace and kinematics cable/end-effector interference constraints.

Considering both statics workspace and kinematics cable/end-effector interference constraints, the **BEST** design was not able to satisfy our design goal of a minimum limiting angle of $\phi_{TC} = 45^\circ$ over the entire *XY* workspace. It does come close to 45° in the middle of the workspace, from the upper-left corner to the lower-right corner, but this is the maximum limiting angle rather than the minimum limiting angle. The **WORST** design angle results (Fig. 10b) are not greatly different from the **BEST** design angle results (Fig. 9b); however, the **BEST** case is clearly preferable. In Figs. 9b and 10b the cable/end-effector interference constraint dominates.

Considering only the statics workspace constraint, there is a much larger difference between the best and worst cases (not shown since this is impractical). Many cases can exceed the desired angle of 45° if we ignore the interference constraint (for instance, the general case of Figs. 4 exceeds this goal in most of the XY statics workspace). Interestingly, the **BEST** case identified above for both statics workspace and cable/end-effector interference constraints is nearly the worst case considering statics workspace only! However, we cannot ignore the interference constraint and so we propose the results given above as the **BEST** and **WORST** cases.

It is possible that, through clever design to minimize the chance of cable/end-effector interference, one could increase the effective overall planar CDDR workspace. It was the intent of our work to remain conservative in design. Reducing cable/end-effector interference is a topic for further work.

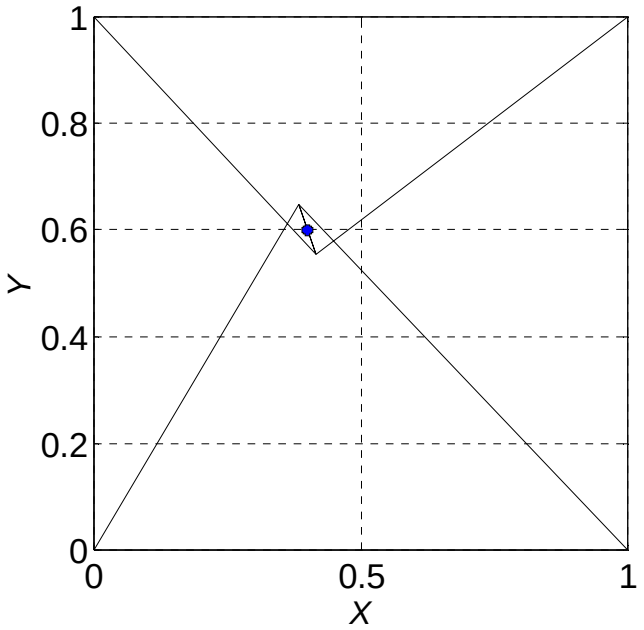

Figure 9a. Best Design a = 0, b = 0.1

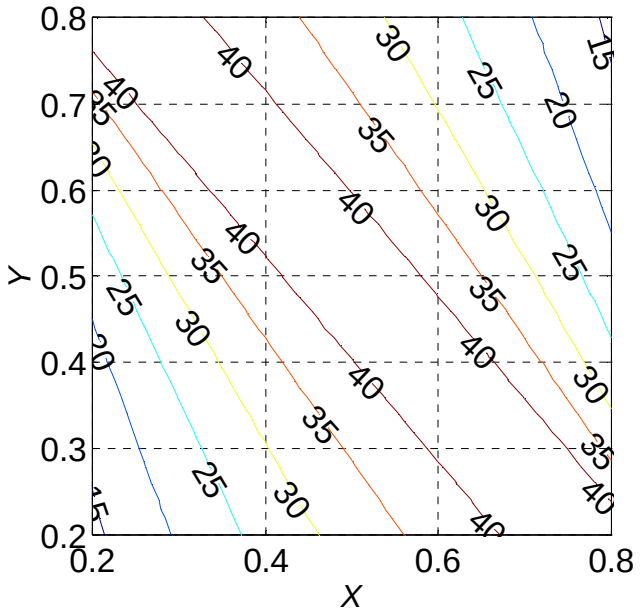

Figure 9b. Best Limiting ϕ_{TC} Results (deg)

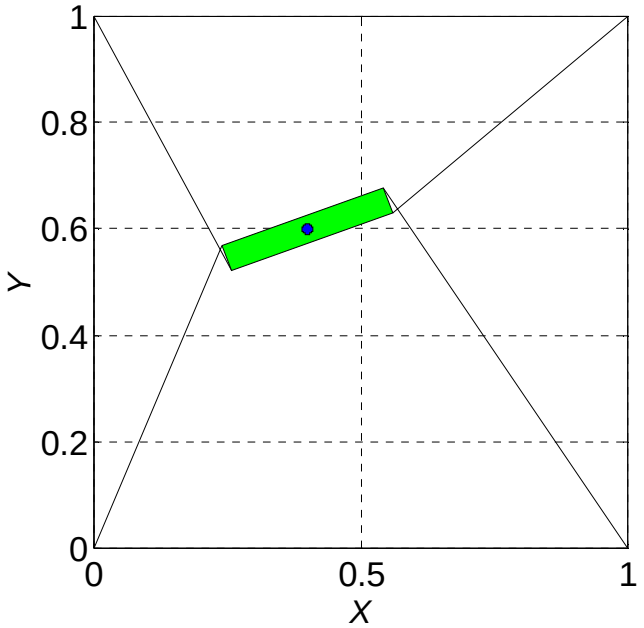

Figure 10a. Worst Design a = 0.32, b = 0.05

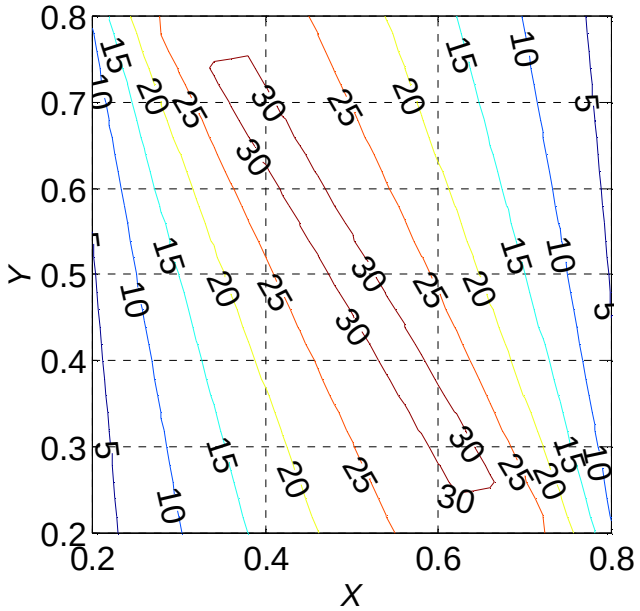

Figure 10b. Worst Limiting ϕ_{TC} Results (deg)

The **BEST** and **WORST** results presented are not general but subject to our design parameters (c=1 and a,b limited to discrete values as explained previously) and our design criteria (we want the largest statics workspace possible; over all XY we wish the largest limiting ϕ angle wherein all cable tensions may remain only positive).

CONCLUSION

This article presented design of planar cable-direct-driven robots (CDDRs) with one degree of actuation redundancy, with regard to best statics workspace for general wrench exertion and with regard to kinematic cable/end-effector interference. The results may be extended to other cable-direct-driven robots and haptic interfaces (CDDHIs) with one degree of actuation redundancy that must exert various wrenches on the environment and the human hand. Statics workspace is defined as that workspace in which *all possible wrenches* may be applied with only positive cable tensions. The well-known particular and homogeneous solution from kinematically-redundant manipulator rate control was adapted to calculate the tension control for exerting commanded wrenches. A simple method was presented to determine the limits of the statics workspace. Using this method and the cable/end-effector interference determination method presented, the best and worst planar 4-cable CDDR designs were found, subject to our design parameters and design criteria. The cable/end-effector interference constraint was found to dominate. Future work plans include developing designs to minimize the cable/end-effector interference problem and to implement and evaluate our CDDR and CDDHI designs in hardware. Potential applications of this technology include industrial robot tasks (assembly, welding, painting, etc.), large-scale outdoor robots (e.g. construction and shipyards), and haptic interfaces.

REFERENCES

J.S. Albus, R. Bostelman, and N.G. Dagalakis, 1993, *"The NIST ROBOCRANE"*, Journal of Robotic Systems, 10(5): 709-724.

G.C. Burdea, 1996, Force and Touch Feedback for Virtual Reality, John Wiley & Sons, New York.

P.D. Campbell, P.L. Swaim, and C.J. Thompson, 1995, "*Charlotte Robot Technology for Space and Terrestrial Applications*", 25th International Conference on Environmental Systems, San Diego, SAE Article 951520.

C.M. Gosselin, 1996, "Parallel Computation Algorithms for the Kinematics and Dynamics of Planar and Spatial Parallel Manipulators", *Journal of Dynamic Systems, Measurement, and Control*, 118(1): 22-28.

M. Ishii and M. Sato, 1994, *"A 3D Spatial Interface Device Using Tensed Strings"*, Presence-Teleoperators and Virtual Environments, MIT Press, Cambridge, MA, 3(1): 81-86.

S. Kawamura and K. Ito, 1993, *"New Type of Master Robot for Teleoperation Using a Radial Wire Drive System"*, Proceedings of the IEEE/RSJ International Conference on Intelligent Robots and Systems, Yokohama, Japan, July 26-30, 55-60.

R. Lindemann and D. Tesar, 1989, *"Construction and Demonstration of a 9-String 6-DOF Force Reflecting Joystick for Telerobotics"*, NASA International Conference on Space Telerobotics, (4): 55-63.

R.G. Roberts, T. Graham, and J.M. Trumpower, 1997, "*On the Inverse Kinematics and Statics of Cable-Suspended Robots*", IEEE International Conf. on Systems, Man, and Cybernetics, Orlando, FL.

Y. Shen, H. Osumi, and T. Arai, 1994, *"Manipulability Measures for Multi-wire Driven Parallel Mechanisms"*, IEEE International Conference on Industrial Technology, 550-554.

D. Stewart, 1966, *"A Platform with Six Degrees of Freedom"*, Proceedings of the Institute of Mechanical Engineers (London), 180(15): 371-386.

L.W. Tsai, 1999, Robot Analysis: The Mechanics of Serial and Parallel Manipulators, Wiley, New York.

R.L. Williams II, 1998, *"Cable-Suspended Haptic Interface"*, International Journal of Virtual Reality, 3(3): 13-21.